Reverberation Chamber Techniques for Determining the Radiation and Total Efficiency of Antennas

Christopher L. Holloway, *Fellow, IEEE*, Haider A. Shah, Ryan J. Pirkl, *Member, IEEE*, William F. Young, *Member, IEEE*, David A. Hill, *Life Fellow, IEEE*, and John Ladbury, *Member, IEEE*

***Abstract*—Reverberation chambers are becoming a popular alternative testing facility for a wide range of electromagnetic applications. Because of the statistical environment created inside a reverberation chamber, they offer a unique test facility. In particular, these chambers are ideally suited for performing radiated power measurements of either an antenna or device under test, and as such, it is possible to determine the efficiency of antennas. There have been several reverberation chamber techniques proposed over the years for measuring the antenna efficiency; however, these techniques require either the use of a reference antenna (i.e., an antenna with a known efficiency) and/or require the assumption that the two antennas used in the test have identical efficiencies. In this paper, we present three different approaches for determining both the radiation and total efficiencies of an unknown antenna that overcome these limitations and assumptions. We present a one-antenna approach, a two-antenna approach, and a three-antenna approach. We present measured data for three different antennas in order to compare these three approaches. We also discuss the uncertainties related to these types of measurements.**

***Index Terms*—Antenna measurements, antenna radiation efficiency, reverberation chambers, total efficiency, uncertainties.**

I. Introduction

A REVERBERATION chamber (RC) is basically a shielded room (metallic walls) with an arbitrarily-shaped metallic rotating paddle (stirrer or tuner) [1]. The paddle is designed to be non-symmetric and is used to create a continuously changing boundary condition of the electromagnetic fields in the chambers. Rotating the paddle creates a statistical environment in a reverberation chamber and this statistical environment offers a unique test facility. Electromagnetic reverberation chambers are becoming popular as an alternative test facility for both electromagnetic and electromagnetic compatibility measurements. Reverberation chambers were initially used in acoustics for various applications [2], but then later emerged in the electromagnetic community where they were first used as high-field amplitude test facilities for electromagnetic interference and compatibility. Reverberation chambers are currently used for a wide range of other measurement applications. Applications include: (1) radiated immunity of components and large systems; (2) radiated emissions; (3) shielding characterizations of cables, connectors, and materials; (4) antenna measurements (including efficiency); (5) probe calibration; (6) characterization of material properties, (7) absorption and heating properties of materials; (8) biological and biomedical effects; (9) testing wireless devices; and (10) simulating various wireless multipath environments (see [1] and [3] for a list of papers covering the different applications).

In this paper we are concerned with determining both the total efficiency (defined as the ratio of the power radiated to the power available at the antenna port) and the radiation efficiency (defined as the ratio of the power radiated to the power accepted by the antenna port). In the area of efficiency measurements, there have been several reverberation chamber techniques proposed over the years [1], [4]–[9]. The problem with these approaches is that they either require the use of a reference antenna (i.e., an antenna with a known efficiency) and/or require one to assume that the two antennas used in the test to have identical characteristics (or identical efficiencies). One exception is the technique given in [10]–[12] where a Wheeler cap type approach is proposed (one basically compares the reflection coefficient measurements of an antenna made in free-space to those made in a RC), which has its own approximations and limitations.

One common approach (used in the IEC standard [8]) is to place a reference antenna (an antenna with a known efficiency, $A_{\rm ref}$ in Fig. 1) inside a chamber along with a generic receiving antenna (A_{Rx}, see Fig. 1). The received power at the receiving antenna with the reference antenna used as a transmitting antenna is measured and is referred to as $P_{\rm ref}$. The reference antenna is replaced with an antenna under test (AUT in Fig. 1) and the received power is measured again (referred to as $P_{\rm AUT}$). The total efficiency of the AUT, relative to the efficiency of the reference antenna is given by:

$$\eta_{\rm AUT,relative} = \frac{P_{\rm AUT}}{P_{\rm ref}} \tag{1}$$

and the absolute efficiency is given by

$$\eta_{\rm AUT} = \frac{P_{\rm AUT}}{P_{\rm ref}}\eta_{\rm ref} \tag{2}$$

where $\eta_{\rm ref}$ is the efficiency of the reference antenna. This approach requires the knowledge of the efficiency of the reference antenna. On the other hand, if one assumes two identical antennas are used for the transmitting and receiving antennas, then the efficiency for the two identical antennas can be obtained

Manuscript received May 31, 2011; revised August 18, 2011; accepted October 01, 2011. Date of publication January 31, 2012; date of current version April 06, 2012.

The authors are with the National Institute of Standards and Technology, Electromagnetics Division, U.S. Department of Commerce, Boulder Laboratories, Boulder, CO 80305 USA (e-mail: holloway@boulder.nist.gov).

Color versions of one or more of the figures in this paper are available online at http://ieeexplore.ieee.org.

Digital Object Identifier 10.1109/TAP.2012.2186263

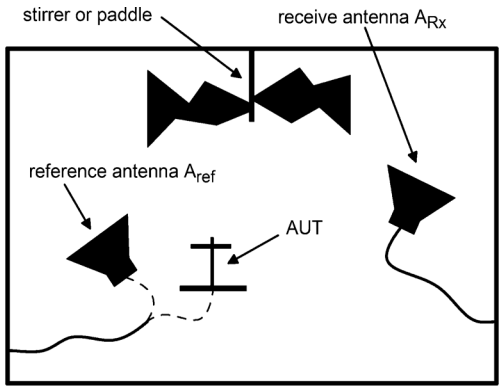

Fig. 1. RC set-up for the measurement of the efficiency for an AUT using a reference antenna.

without a known reference antenna. This approach is discussed next.

The one parameter that is often used to characterize a reverberation chamber is the quality factor (Q), and is defined as [1]

$$Q = \frac{\omega U}{P_d} \tag{3}$$

where U is the energy stored in the chamber, P_d is the power dissipated in the chamber, and $\omega = 2\pi f$ (where f is the frequency). In the past, individuals have used both time-domain and frequency-domain data to determine this Q. In the frequency domain, Q is usually obtained through a measurement of power inside the chamber (see [1] for details). In the time domain one usually first determines the chamber time constant or chamber decay time $(\tau_{\rm RC})$, see [13] and [14] for a discussion on these types of measurements. The chamber decay time is directly related to the losses in the chamber and, more importantly, is related to the chamber Q by the following [1]:

$$Q = \omega\, \tau_{\rm RC} \tag{4}$$

where $\tau_{\rm RC}$ is the chamber decay time or chamber time constant [1]. However, in some situations (depending on the chamber size and the antennas used), there is a systematic offset when comparing Q obtained from time-domain and frequency-domain measurements. Time-domain estimates of Q are higher than those obtained in the frequency-domain. For example, see Fig. 6 in [13] and Figs. 7.13 and 11.1 in [1].

The difference in the Q obtained in the time domain to that obtained in the frequency domain can be attributed to the efficiencies of the antennas used in the measurement. At high enough frequencies and high chamber loss conditions, $\tau_{\rm RC}$ (and the corresponding Q obtained from (4)) is dominated by the wall (and paddle) losses in the chamber, see (10) in [13]. However, Q obtained with the usual frequency-domain power measurements has effects due to both the wall (and paddle) losses in the chamber and to loss in the antenna (both ohmic and dielectric losses), and as such Q from a frequency-domain measurement will be smaller than that obtained from a chamber time-constant calculation [i.e., a time-domain measurement obtained from (4)], which is consistent with the results presented is Fig. 6 in [13], in Figs. 7.13 and 11.1 in [1].

As stated, the difference between these two Q determinations is directly related to the efficiencies of the antennas used in the measurements and is seen by considering the two antennas placed in the chamber depicted in Fig. 2. Antenna A is connected to port 1 of a vector network analyzer (VNA) via a cable running through the bulkhead of the chamber, and antenna B is connected to port 2 of the VNA via another cable running through the bulkhead of the chamber. Antenna A is used to couple energy into the chamber and is referred to as the transmitting antenna, and antenna B is the receiving antenna. The power that is radiated into the chamber is referred to as P_{TX}. Once this energy gets into the chamber, a portion is dissipated in the chamber walls and paddle $(P_{\rm RC})$, a portion of the energy reflects off the chamber walls and paddle and is captured by the receiving antenna (this power is referred to as P_{RX}), and a portion of the energy reflects off the chamber walls and paddle and is captured by the transmitting antenna (this power is referred to as P_{rf}). Because the antennas at the two ports are not ideal antennas, the power levels inside the chamber are not the power levels at the input port of the antennas. It is easy to show that

$$P_{TX} = \eta_A^{total} P_1, \quad P_{RX} = \frac{P_2}{\eta_B^{\rm total}}, \text{ and } P_{rf} = \frac{P_3}{\eta_A^{\rm total}} \tag{5}$$

where $\eta_A^{\rm total}$ and $\eta_B^{\rm total}$ are the total efficiencies of the antennas at ports 1 and 2, respectively. P_1 is the forward power being delivered to the antenna port 1, P_2 is the power at the output port of antenna port 2, and P_3 is the output power of antenna port 1, see Fig. 2. We have assumed that all losses in the cables (up to the antenna ports) have been calibrated out through standard calibration techniques. In [1] it is shown that if we assume the RC is a so-called "well performing" chamber (which implies the chamber is well stirred with a large number of modes and a high mode density), we have the following:

$$\frac{\langle P_{RX}\rangle}{P_{TX}} = \frac{1}{C_{\rm RC}} Q \tag{6}$$

where Q is the quality factor of the chamber, $\langle P_{RX}\rangle$ is the average received power, P_{TX} is the transmitted power in the chamber. The symbol $\langle\,\rangle$ represents an ensemble average. The parameter $C_{\rm RC}$ is a chamber constant defined as

$$C_{\rm RC} = \frac{16\pi^2 V}{\lambda^3} \tag{7}$$

where V is the volume of the chamber, and λ is the free-space wavelength. In the RC, the ensemble average is obtained from different independent samples, where these samples are obtained by different paddle (or stirring) positions, averaging of a "small" band of frequencies, and/or measuring the power at different locations in the chamber. The left side of (6) can be replaced with the use of the expressions in (5) to give

$$\eta_A^{\rm total}\eta_B^{\rm total} = C_{\rm RC}\frac{\langle P_2\rangle}{P_1}\frac{1}{Q}. \tag{8}$$

If we assume a standard calibration procedure is performed before the measurement, any losses in the cable are removed from the measurements and as such it can be shown in [16] that the

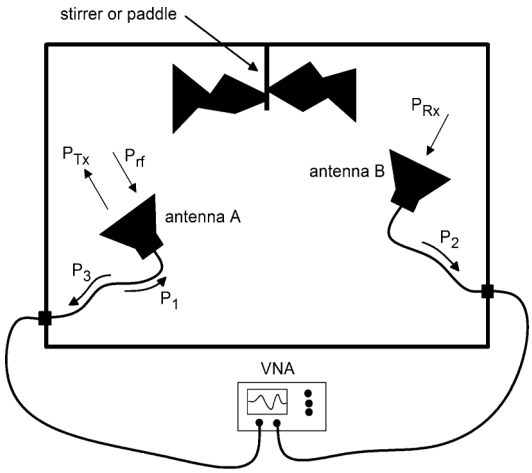

Fig. 2. RC set-up for the two-antenna measurement method for determining the antenna efficiency.

second term in the right hand side of the expression is related to the S-parameter measured on the VNA as

$$\frac{\langle P_2\rangle}{P_1} = \langle |S_{21}|^2\rangle. \tag{9}$$

A simple measurement of this S-parameter would have contributions from the stirred (energy that interacts with the paddle) and unstirred energy (energy that does not interact with the paddle, including line-of-sight (LOS) and non-LOS energy) inside the chamber, see [3] and [16] for details. The assumption inherent in deriving (8) and (9), is that the unstirred contributions are removed from measurements of S_{21}. A discussion on how this is accomplished is given in Section 5. The product of the two efficiencies of the two antennas can now be expressed as:

$$\eta_A^{\text{total}}\,\eta_B^{\text{total}} = C_{\text{RC}}\,\langle |S_{21}|^2\rangle \frac{1}{Q}. \tag{10}$$

From this expression, we only have an equation for the product of the two unknown efficiencies (η_A^{total} and η_B^{total}), and are expressed in terms of two unknowns, $\langle |S_{21}|^2\rangle$ and Q. While $\langle |S_{21}|^2\rangle$ can be obtained from a VNA measurement, we still need Q.

The first two terms on the right side of (10) are recognized as the commonly used expression to determine Q from frequency-domain data for a chamber with ideal antennas, and hence is defined as the *"frequency-domain" Q* given by (see [1] for details of this a definition):

$$Q_{\text{FD}} = C_{\text{RC}}\langle |S_{21}|^2\rangle. \tag{11}$$

The problem with this common approach for determining the chamber Q is that the antenna effects (i.e., losses) are included in this measurement and is only a measurement of the "true" chamber Q when the antennas are ideal. The last term in this expression (i.e., $1/Q$) can be thought of as the *"time-domain" Q* since it is expressed in terms of the chamber decay time, as shown in (4). Thus, one could say that the product of the two efficiencies are simply a ratio of the *"frequency-domain" Q_{FD}* to the *"time-domain" Q_{TD}*, or

$$\eta_A^{\text{total}}\,\eta_B^{\text{total}} = \frac{Q_{\text{FD}}}{Q_{\text{TD}}} \tag{12}$$

where Q_{FD} and Q_{TD} are the chamber quality factors obtained from a frequency-domain and time-domain measurement, respectively. If the antennas are ideal, then this ratio is theoretically equal to one.

Equation (10) can be rewritten by noting that Q in this expression is associated with only the losses of the chamber (not losses associated with the antennas) as such, from (4), Q is related the chamber decay constant τ_{RC} (through (4)), and hence (10) can be expressed as

$$\eta_A^{\text{total}}\eta_B^{\text{total}} = \frac{C_{\text{RC}}}{\omega}\langle |S_{21}|^2\rangle \frac{1}{\tau_{\text{RC}}}. \tag{13}$$

With that said, we still need two pieces of information, $\langle |S_{21}|^2\rangle$ and τ_{RC}, in order to determine the product of the efficiencies of the two antennas. If these two quantities are measured we still have the problem that only the product of the two efficiencies are obtained. If we assume the antennas are identical, then the efficiency of each antenna is determined. Reference [4] uses a similar formulation for determining the efficiencies of two identical antennas, in which the chamber decay time (τ_{RC}) is obtained by turning a source on-and-off. In a later section we discuss how τ_{RC} is obtained with an inverse Fourier transform of frequency-domain measurements. Regardless, the problem with this formulation is that one must assume the two antennas are identical.

Let us turn our attention back to the term we call the antenna efficiency $\eta_{A,B}$. We need to be clear what type of efficiency this term is referring to. As stated in either (10) or (13), this is the total overall efficiency of the antenna (defined as the ratio of the power radiated to the power available at the antenna port), or the efficiency related to both radiation efficiency (ohmic and dielectric losses in the antenna) and antenna reflection or mismatch efficiency, as defined in [18]. As we will discuss later, it is possible to correct S_{21} for the antenna mismatch, and as such obtain expressions for the radiation efficiency of the antenna (defined as the ratio of the power radiated to the power accepted by the antenna port) related to ohmic and/or dielectric losses in the antenna.

In this paper we present techniques that overcome these limitations and assumptions to allow the determination of both the overall (or total) efficiency and radiation efficiency of the antennas. We will present three techniques for determining the efficiency of an antenna that do not require either the use of a reference antenna (i.e., an antenna with a known efficiency) nor requires one to assume that the two antennas used in the test have identical efficiencies. We present a one-antenna approach, a two-antenna approach, and a three-antenna approach. These techniques are derived by following a similar procedure to that used in deriving (13). We present experimental data for three different antennas (one monopole antenna and two different horn antennas). Finally, we discuss the measurement uncertainties associated with the these types of antenna efficiency measurements. Of the three techniques presented here, the

three-antenna approach requires the fewest assumptions of the three, in that it overcomes the inherent assumptions (as discussed below) made in both the one-antenna and two-antenna approaches.

Finally, we need to emphasize that the techniques presented in this paper assumes that the losses in the chamber are dominated by the chamber wall losses (and possible rf absorber losses if they are used in the chamber, see [13]) when compared to energy pulled out of the chamber by the antennas used in the measurements. This is usually the case for reverberation chambers operating above 800 MHz. When chamber wall losses are not dominant when compared to antenna losses, determining the chamber decay constant $(\tau_{\rm RC})$ can become problematic. When wall losses are not dominant, antenna losses can influence the determination of $\tau_{\rm RC}$ (which should only be a parameter of the chamber and not of the antennas). Under these conditions, the techniques presented here need to be modified and this is the topic of a future publication.

II. One-Antenna Approach

It is possible to determine the efficiency from the S_{11} of a single antenna placed inside a chamber. However, this approach requires one to make an assumption about the relationship between a one-port and two-port VNA measurement. This approach requires a few modifications to the discussion given above. Consider one antenna placed in the chamber depicted in Fig. 3. Antenna A is connected to port 1 of a vector network analyzer (VNA) via a cable running through the bulkhead of the chamber, and this antenna is used to couple energy into the chamber. Once this energy gets into the chamber, a portion is dissipated in the chamber walls and paddle $(P_{\rm RC})$ and a portion of the energy reflects off the chamber walls and paddle and is captured by the antenna (this power is referred to as P_{rf}). Because the antenna at port 1 is not an ideal antenna, the power levels inside the chamber are not the power levels at the input of antenna port 1 (relative to the cable), and subsequently propagates along the cable that connect the antenna to the VNA. It is easy to show that

$$P_{TX} = \eta_A^{\rm total} P_1 \quad \text{and} \quad P_{rf} = \frac{P_3}{\eta_A^{\rm total}}. \tag{14}$$

Once again, it is assumed that all losses in the cables (up to the antenna port) have been calibrated out through standard calibration techniques (the uncertainties associated with this are included in the Type B uncertainties as discussed below). Thus, we have

$$\frac{\langle P_{rf}\rangle}{P_{TX}} = \frac{\langle P_3\rangle}{\eta_A^{\rm total}\,\eta_A^{\rm total}\,P_1} = \frac{\langle |S_{11,s}|^2\rangle}{\eta_A^{\rm total}\,\eta_A^{\rm total}} \tag{15}$$

where as before, $\eta_A^{\rm total}$ is the total efficiency of the antenna at port 1 and $\langle |S_{11,s}|^2\rangle = \langle P_3\rangle / P_1$. P_1 is the forward power being delivered to the antenna port 1, and P_3 is the reflected (or output) power of antenna port 1. The quantity $\langle |S_{11,s}|^2\rangle$ represents the stirred energy contribution of S_{11}. As discussed in the introduction, the measured S-parameters used here and those used in the next two sections need to be corrected for the possibility of any unstirred energy contribution. Correcting for the unstirred energy in the S-parameters is a common practice used in reverberation chamber measurements, and the manner in which these contributions are accounted for, is discussed in Section 5.

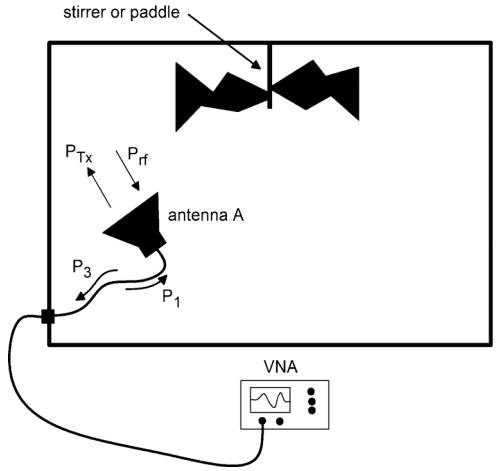

Fig. 3. RC set-up for the one-antenna measurement method for determining the antenna efficiency.

In [1] and [15], Ladbury and Hill show that if we assume the RC is a so-called "ideal" performing chamber (which implies the chamber is well stirred with a large number of modes and a large mode-density) we have the following

$$\langle P_{rf}\rangle = 2\langle P_{RX}\rangle \tag{16}$$

where, as defined above, P_{RX} would be the received power at a receiving antenna inside the chamber (assuming that one is present). This result is analogous to the enhanced backscatter that has been derived for scattering by a random medium. The physical mechanism for this is the coherent addition of rays in the backscatter direction [15], and is the same in both reverberation chambers and in scattering by random media. Using this and rearranging (15) we have

$$\left(\eta_A^{\rm total}\right)^2 = \frac{\langle |S_{11,s}|^2\rangle}{2}\frac{P_{TX}}{\langle P_{RX}\rangle}. \tag{17}$$

Using the expression given in (6), the efficiency for the antenna at port 1 reduces to the following

$$\eta_A^{\rm total} = \sqrt{\frac{\langle |S_{11,s}|^2\rangle}{Q}\frac{C_{\rm RC}}{2}}. \tag{18}$$

Once again, Q is the quality factor associated with loss inside the chamber and not associated with losses in the antenna. As discussed above, Q can be obtained from an estimate based on the chamber time constant $\tau_{\rm RC}$ (see (4)), and as such this expression reduces to

$$\eta_A^{\rm total,1} = \sqrt{\frac{C_{\rm RC}}{2\,\omega}\frac{\langle |S_{11,s}|^2\rangle}{\tau_{\rm RC}}}. \tag{19}$$

Thus, a measurement of $\langle |S_{11,s}|^2\rangle$ and $\tau_{\rm RC}$ is all that is required to determine the efficiency of a single antenna. The first superscript "total" is used to emphasize that this is the total efficiency of this antenna (including both mismatch and radiated efficiencies) and the second superscript "1" is used to emphasize that

one antenna is required in the approach (i.e., the one-antenna approach).

The radiation efficiency can be obtained by correcting the measured S_{11} to account for the antenna mismatch. Using a similar procedure as given in [16] and [17] for correcting mismatch in S_{21}, the correction for $\langle|S_{11}|^2\rangle$ is expressed as

$$\langle|S_{11,s}|^2\rangle_{\rm cor} = \frac{\langle|S_{11,s}|^2\rangle}{(1-|\langle S_{11}\rangle|^2)\,(1-|\langle S_{11}\rangle|^2)}. \tag{20}$$

The term $|\langle S_{11}\rangle|^2$ that appears in the denominator is essentially the free-space reflection coefficient (or S_{11}) of the antenna. In Section 5, we show that $|\langle S_{11}\rangle|^2$ as measured in the reverberation chamber (for a given antenna) is the same as $|S_{11}|^2$ measured in an anechoic chamber. Thus, the radiation efficiency for a single antenna is given by

$$\eta_A^{\rm rad,1} = \sqrt{\frac{C_{\rm RC}}{2\,\omega}\frac{\langle|S_{11,s}|^2\rangle_{\rm cor}}{\tau_{\rm RC}}}. \tag{21}$$

The first superscript "rad" is used to emphasize that this is the radiation efficiency of the antenna (including only ohmic and/or dielectric losses), and the second superscript "1" is used to emphasize that one antenna is required in this approach. In a later section, we discuss how $\tau_{\rm RC}$ is obtained from an S_{11} measurement.

III. Two-Antenna Approach

In the previous section, a one-antenna approach was derived assuming the relation given in (16) is valid in the chamber. If we do not make this assumption, the antenna efficiency can be obtained from a two-antenna approach. Once again, consider the two-antenna setup shown in Fig. 2. From the arguments of the previous two sections, we have:

$$\begin{aligned}
\langle|S_{11,s}|^2\rangle &= \eta_A^{\rm total}\,\eta_A^{\rm total}\frac{\langle P_{rf,1}\rangle}{P_{TX}}\\
\langle|S_{22,s}|^2\rangle &= \eta_B^{\rm total}\,\eta_B^{\rm total}\frac{\langle P_{rf,2}\rangle}{P_{TX}}\\
\langle|S_{21,s}|^2\rangle &= \eta_B^{\rm total}\,\eta_A^{\rm total}\frac{\langle P_{RX}\rangle}{P_{TX}}
\end{aligned} \tag{22}$$

where $P_{rf,1}$ and $P_{rf,2}$ refer to the power that is reflected into the antennas at ports 1 and 2, respectively. Now let us assume the relationship between $P_{rf,1}$ and P_{RX} (and similarly the relationship between $P_{rf,2}$ and P_{RX}) is only known to some constant e_b, or

$$\begin{aligned}
\langle P_{rf,1}\rangle &= e_b\,\langle P_{RX}\rangle\\
\langle P_{rf,2}\rangle &= e_b\,\langle P_{RX}\rangle
\end{aligned} \tag{23}$$

where we use e_b for the constant referring to an enhanced backscatter constant, which is analogous to the enhanced backscatter that has been derived for scattering by random medium. While the two-antenna approach does not require $e_b = 2$ (as was the case for the one-antenna approach), it does require e_b to be identical for antennas placed in different positions within the chamber (i.e., spatial homogeneity in the chamber). Below, we will illustrate how well this assumption holds.

From (22) and (23), we have the following relationship

$$\begin{aligned}
\frac{\langle|S_{11,s}|^2\rangle}{\langle|S_{21,s}|^2\rangle} &= e_b\frac{\eta_A^{\rm total}}{\eta_B^{\rm total}}\\
\frac{\langle|S_{22,s}|^2\rangle}{\langle|S_{21,s}|^2\rangle} &= e_b\frac{\eta_B^{\rm total}}{\eta_A^{\rm total}}.
\end{aligned} \tag{24}$$

We have two equations and two unknowns (the value for e_b and the ratio $\eta_A^{\rm total}/\eta_B^{\rm total}$). The ratio of the unknown efficiencies can be eliminated to obtain the following expression for the unknown e_b:

$$e_b = \frac{\sqrt{\langle|S_{11,s}|^2\rangle\langle|S_{22,s}|^2\rangle}}{\langle|S_{21,s}|^2\rangle}. \tag{25}$$

If the chamber was performing ideally, then $e_b = 2$ (as assumed in the previous section). Using this value of e_b and following a similar procedure as given in the previous section, it can be shown that the total efficiencies of the two antennas is given by

$$\begin{aligned}
\eta_A^{\rm total,2} &= \sqrt{\frac{C_{\rm RC}}{\omega\ e_b}\frac{\langle|S_{11,s}|^2\rangle}{\tau_{\rm RC}}}\\
\eta_B^{\rm total,2} &= \sqrt{\frac{C_{\rm RC}}{\omega\ e_b}\frac{\langle|S_{22,s}|^2\rangle}{\tau_{\rm RC}}}
\end{aligned} \tag{26}$$

where the second superscript "2" is used to emphasize that two antennas are required in this approach (i.e., the two-antenna approach). We can recognize that these two expressions are simply the expression given in (19) with 2 replaced by e_b.

Once S_{11} and S_{22} are corrected for the antenna mismatch, the radiation efficiencies for the two antennas are given by

$$\begin{aligned}
\eta_A^{\rm rad,2} &= \sqrt{\frac{C_{\rm RC}}{\omega\ e_b}\frac{\langle|S_{11,s}|^2\rangle_{\rm cor}}{\tau_{\rm RC}}}\\
\eta_B^{\rm rad,2} &= \sqrt{\frac{C_{\rm RC}}{\omega\ e_b}\frac{\langle|S_{22,s}|^2\rangle_{\rm cor}}{\tau_{\rm RC}}}.
\end{aligned} \tag{27}$$

where $\langle|S_{22,s}|^2\rangle_{\rm cor}$ is given in (20) with S_{11} replaced by S_{22}.

IV. Three-Antenna Approach

The previous two approaches required one to make an assumption about the relationship between $P_{rf,1}$ and P_{RX} (and similar relationships between $P_{rf,2}$ and P_{RX}). The one-antenna approach requires the relationship to be 2. While the two-antenna approach does not require the relationship to be 2, it does require this relationship to be identical for antennas placed in different positions in the chamber. By using three antennas, these assumptions are not required. This three-antenna approach for determining the antenna efficiencies is analogous to the three-antenna approach used to determine the absolute gain without a priori knowledge of the gain of any of the three antennas, see [19].

Consider three antennas placed in the chamber depicted in Fig. 4. Connect any two of these antennas (say antenna A and B) to ports 1 and 2 of a VNA and measure the S-parameters. From (13), we can express the product of the efficiencies of antennas A and B as the following

$$\eta_A^{\rm total}\ \eta_B^{\rm total} = \frac{C_{\rm RC}}{\omega}\ M_{AB} \tag{28}$$

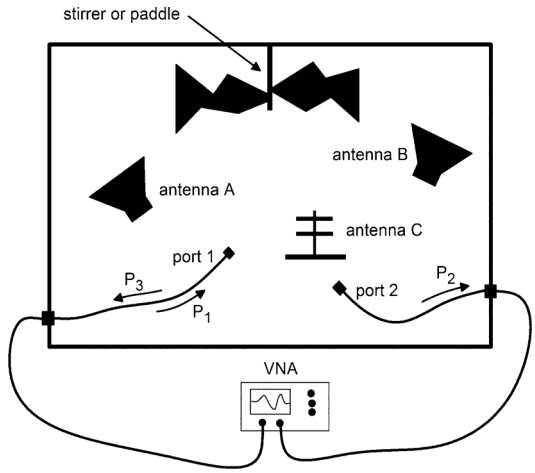

Fig. 4. RC set-up for the three-antenna measurement method for determining the antenna efficiency.

where

$$M_{AB} = \frac{\langle |S_{21,s}|^2 \rangle_{AB}}{\tau_{\mathrm{RC},AB}}. \tag{29}$$

By performing two more sets of similar measurements (one set for antenna A and C, and one set for antennas B and C), we can show that

$$\begin{aligned} \eta_A^{\mathrm{total}}\, \eta_C^{\mathrm{total}} &= \frac{C_{\mathrm{RC}}}{\omega}\, M_{AC} \\ \eta_B^{\mathrm{total}}\, \eta_C^{\mathrm{total}} &= \frac{C_{\mathrm{RC}}}{\omega}\, M_{BC} \end{aligned} \tag{30}$$

where

$$\begin{aligned} M_{AC} &= \frac{\langle |S_{21,s}|^2 \rangle_{AC}}{\tau_{\mathrm{RC},AC}} \\ M_{BC} &= \frac{\langle |S_{21,s}|^2 \rangle_{BC}}{\tau_{\mathrm{RC},BC}}. \end{aligned} \tag{31}$$

If τ_{RC} is truly only a function of the chamber size and the losses in the chamber (not including the loss of the antennas), then we should have

$$\tau_{\mathrm{RC},AB} = \tau_{\mathrm{RC},AC} = \tau_{\mathrm{RC},BC}. \tag{32}$$

This assumption is verified in the next section, and is part of the measurement uncertainty analysis given below. Thus, differences in M_{AB}, M_{AC}, and M_{BC} are a consequence of the characteristics of the three different antennas not being identical (i.e., difference in the antenna efficiencies of the three antennas).

The expressions in (28) and (30) represent three equations and three unknowns (η_A, η_B, and η_C), which can be solved to give the total efficiency for the three unknown antennas as

$$\begin{aligned} \eta_A^{\mathrm{total},3} &= \sqrt{\frac{C_{\mathrm{RC}}}{\omega}} \sqrt{\frac{M_{AB}\, M_{AC}}{M_{BC}}} \\ \eta_B^{\mathrm{total},3} &= \sqrt{\frac{C_{\mathrm{RC}}}{\omega}} \sqrt{\frac{M_{BC}\, M_{AB}}{M_{AC}}} \\ \eta_C^{\mathrm{total},3} &= \sqrt{\frac{C_{\mathrm{RC}}}{\omega}} \sqrt{\frac{M_{AC}\, M_{BC}}{M_{AB}}} \end{aligned} \tag{33}$$

where the second superscript "3" is used to emphasize that three antennas are required in this approach (i.e., the three-antenna approach). The radiation efficiency for the three antennas is obtained by correcting the S-parameters for mismatch and can be obtained from the following

$$\begin{aligned} \eta_A^{\mathrm{rad},3} &= \sqrt{\frac{C_{\mathrm{RC}}}{\omega}} \sqrt{\frac{M_{AB,\mathrm{cor}}\, M_{AC,\mathrm{cor}}}{M_{BC,\mathrm{cor}}}} \\ \eta_B^{\mathrm{rad},3} &= \sqrt{\frac{C_{\mathrm{RC}}}{\omega}} \sqrt{\frac{M_{BC,\mathrm{cor}}\, M_{AB,\mathrm{cor}}}{M_{AC,\mathrm{cor}}}} \\ \eta_C^{\mathrm{rad},3} &= \sqrt{\frac{C_{\mathrm{RC}}}{\omega}} \sqrt{\frac{M_{AC,\mathrm{cor}}\, M_{BC,\mathrm{cor}}}{M_{AB,\mathrm{cor}}}} \end{aligned} \tag{34}$$

where

$$\begin{aligned} M_{ij,\ \mathrm{cor}} &= \frac{\langle |S_{21,s}|^2 \rangle_{ij,\ \mathrm{cor}}}{\tau_{\mathrm{RC},ij}} \\ &= \frac{1}{\tau_{\mathrm{RC},ij}} \frac{\langle |S_{21,s}|^2 \rangle_{ij}}{(1 - |\langle S_{11} \rangle|^2)\,(1 - |\langle S_{22} \rangle|^2)} \end{aligned} \tag{35}$$

where i and j are A, B, or C.

V. Experimental Results

In this section we compared the three proposed techniques to obtain the efficiencies of three different antennas. The three antennas are labeled antennas A, B, and C. Antenna A is a brass-colored dual-ridge horn antenna with an aperture dimension of 13.5 cm by 22.5 cm, see Fig. 5(a), and Antenna B is a second manufacturer's dual-ridge horn antenna (silver in color) with an aperture dimension of 13.5 cm by 24.5 cm, see Fig. 5(b). The two side flanges of Antenna B are constructed with printed circuit board material, while the two side flanges of Antenna A are constructed of brass rods. Antenna C is a 9 cm monopole antenna mounted to a 45.5 cm square copper ground plane, see Fig. 5(c). These three antennas were placed in the National Institute of Standards and Technology (NIST) reverberation chamber with dimensions of 2.9 m by 4.2 m by 3.6 m, see Fig. 6. We performed three sets of measurements, where each set of measurements used two different antenna combinations. For example, antennas A and B were connected to ports 1 and 2 respectively of the VNA, and $S_{11,A}, S_{22,B}$, and $S_{21,AB}$ were measured. Note that $S_{11,A}$ corresponds to the reflection measurement for antenna A connected to port 1, and similarly for $S_{22,B}$. Similarly, a set of measurements for antennas A and C were performed to obtain $S_{11,A}$, $S_{22,C}$, and $S_{21,AC}$ and a set of measurements for antennas B and C were performed to obtain $S_{11,B}$, $S_{22,C}$, and $S_{21,BC}$.

The three techniques require either a measurement of $\langle |S_{11}|^2 \rangle$, $\langle |S_{22}|^2 \rangle$, and/or $\langle |S_{21}|^2 \rangle$. A simple measurement of one of these three S-parameters would have contributions from the stirred energy (energy that interacts with the paddle) and unstirred energy (energy that does not interact with the paddle, including line-of-sight (LOS) and non-LOS energy) inside the chamber, see [3] and [16] for details. With that said, the chamber insertion loss S_{21} can be expressed as a sum of the unstirred component and a component associated with the stirred energy in the chamber as the following

$$S_{21} = S_{21,s} + S_{21,us} \tag{36}$$

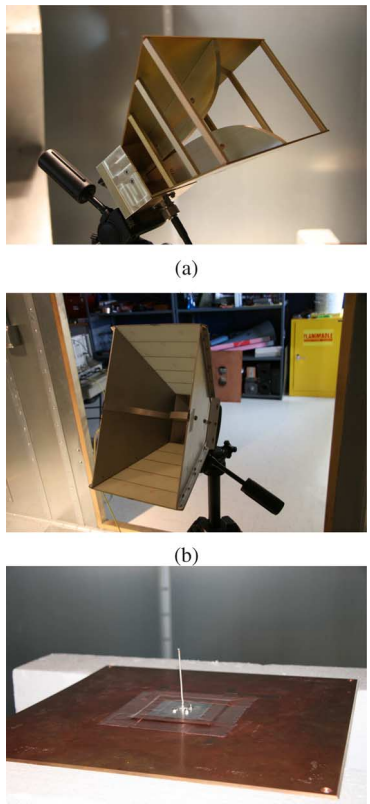

(a) (b) (c)

Fig. 5. The three antennas used in this investigation, (a) antenna A: dual-ridge brass colored horn, (c) antenna B: 2nd model of dual-ridge horn (silver in color), and (c) antenna C: monopole.

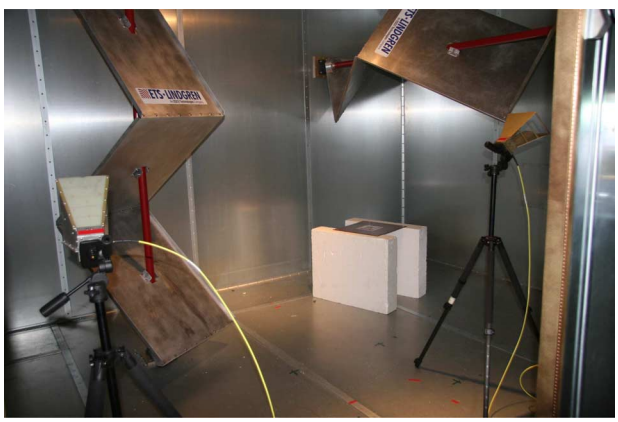

Fig. 6. RC set-up for antenna A, antenna B, and antenna C.

where $S_{21,s}$ is the stirred component and $S_{21,us}$ is the unstirred component. The derivation for $\langle P_{Rx}\rangle/P_{Tx}$ given in [1], (6), assumes that $\langle P_{Rx}\rangle$ has only contributions from the stirred energy inside the chamber. From the previous expression, the contribution from the stirred component can be expressed as

$$\langle|S_{21,s}|^2\rangle = \langle|S_{21} - S_{21,us}|^2\rangle. \tag{37}$$

In [3] and [16] it is shown that

$$S_{21,us} = \langle S_{21}\rangle. \tag{38}$$

Thus, the S-parameters associated with the stirred energy (needed in all three of the proposed antenna techniques) is given by [3] and [16]

$$\langle|S_{21,s}|^2\rangle = \langle|S_{21} - \langle S_{21}\rangle|^2\rangle \tag{39}$$

with similar expressions for $\langle|S_{11,s}|^2\rangle$ and $\langle|S_{22,s}|^2\rangle$.

All of these techniques require knowledge of the chamber decay time (τ_{RC}), which can be obtained from either S_{11} (for the one- and two-antenna approaches) or S_{21} (for the three antenna approach). Details for determining τ_{RC} are found in [13] and [14], which first requires one to obtain the power delay profile for the chamber and is expressed as

$$\mathrm{PDP}(t) = \langle|h(t,n)|^2\rangle \tag{40}$$

where the ensemble average is taken over n, which represents the different independent samples (obtained from paddle stirring, frequency stirring, and/or position stirring). In this expression, $h(t,n)$ is the impulse response of the chamber for different samples n, and is the inverse Fourier transform (IFT) of either S_{11} or S_{21} (depending on which of the three techniques is used), that is,

$$\begin{gathered} h(t,n) = \mathrm{IFT}\left[S_{21_n}(f)\right] \\ \text{or} \\ h(t,n) = \mathrm{IFT}\left[S_{11_n}(f)\right]. \end{gathered} \tag{41}$$

Once the $\mathrm{PDP}(t)$ is obtained, τ_{RC} is determined by recognizing that if the chamber is truly exponential for late-time behavior (see [1]) then the slope of $\ln[\mathrm{PDP}(t)]$ would be $1/\tau_{\mathrm{RC}}$. One could also determine the rms delay spread of $\mathrm{PDP}(t)$ (as was done in [13] and [14]) to determine τ_{RC}. The time constant τ_{RC} should only be a function of the chamber and neither a function of the antenna used to measure it nor a function of whether S_{11} or S_{21} was used. This is illustrated in Fig. 7 where we plot τ_{RC} obtained with the different antennas and from $h(t,n)$ obtained from the use of either S_{11} or S_{21}. This figure shows consistent results when we compare τ_{RC} obtained from the different methods and/or different antennas. These differences manifest themselves in the measurement uncertainties of the antenna efficiency. This point is discussed in the next section.

Fig. 8–10 show the radiation efficiency determined from the different techniques for each of the three antennas, i.e., correcting for antenna mismatch in the S-parameters. Fig. 8 shows the results for antenna A (the brass-colored horn antenna). In this figure we see that the one-antenna approach estimates a higher efficiency as compared to the other approaches. This overestimate is due to the fact that $e_b \neq 2$ (discussed below). Once the value of e_b is corrected (as is done in the two-antenna approach) we see very little difference between the two-antenna and three-antenna approaches. The differences are well within the measurement uncertainties, as discussed in the next section. Fig. 9 shows the results for antenna B (the silver horn antenna). Similar to the results for antenna A, we see that the one-antenna approach overestimates the efficiency when compared to the other approaches, due in part to $e_b \neq 2$. Fig. 10 shows the results for antenna C (the monopole antenna). Once again we see that the results from the one-antenna approach overestimate

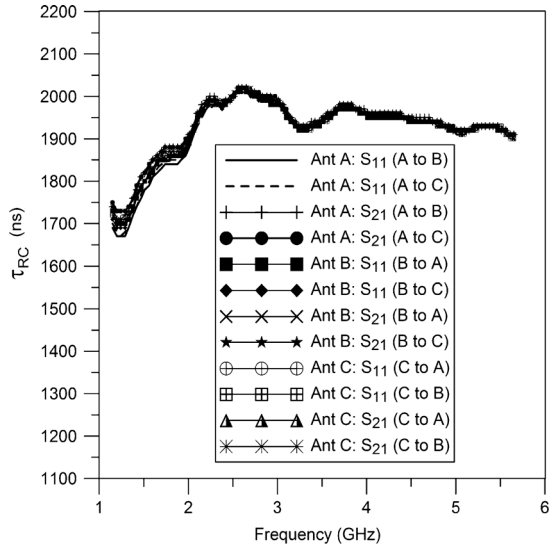

Fig. 7. Measured τ_{RC} obtained from twelve different sets of data.

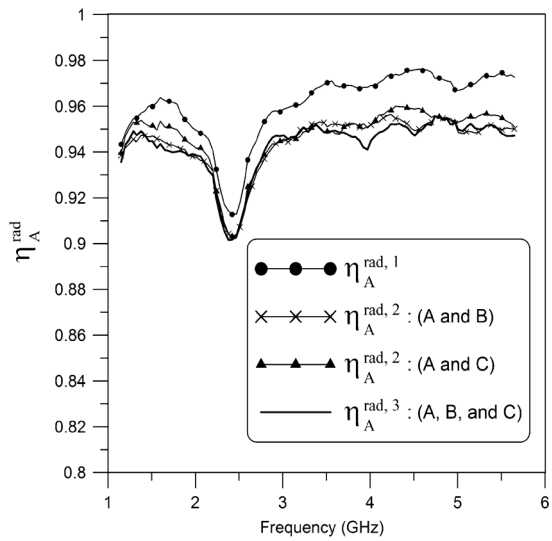

Fig. 8. Radiation efficiency: a comparison of the three different approaches for antenna A.

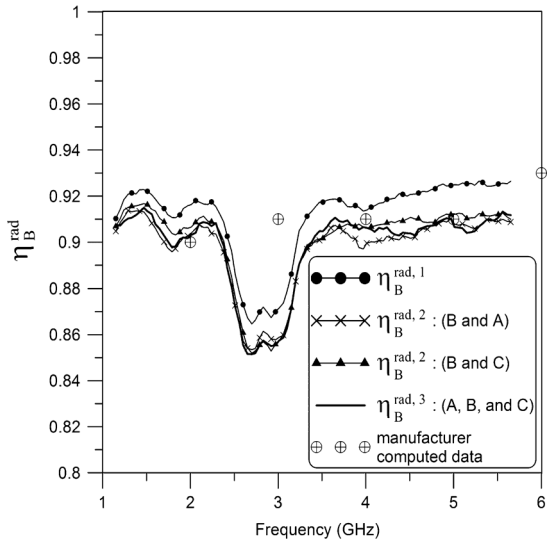

Fig. 9. Radiation efficiency: a comparison of the three different approaches for antenna B.

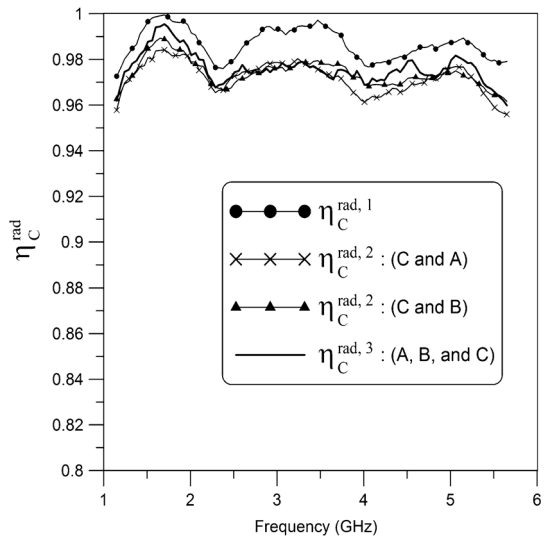

Fig. 10. Radiation efficiency: a comparison of the three different approaches for antenna C.

the results obtained from the three-antenna approach, while the two-antenna and three-antenna approaches give similar results.

To validate these techniques we need an independent measurement or estimate of the radiation efficiencies of these three antennas. Unfortunately, we only have radiation efficiency data for antenna B for which we can compare our results. The manufacturer of antenna B has estimated the radiation efficiency of the silver dual-ridge horn to be approximating 91% in the 1 GHz to 6 GHz frequency range. The manufacturer data was obtained from a numerical calculation of the antenna efficiency, in which the actual material properties (in this case aluminum) of the antenna where used in the simulation. These results are consistent with the results shown in Fig. 9.

By not correcting for the mismatch between the antenna feed and the cable, the total efficiency (the mismatch efficiency plus radiation efficiency) can be determined. Fig. 11–13 show the total efficiency determined from the different techniques for each of the three antennas. These results show the classic oscillations seen in results when mismatches are present.

Fig. 14 compares the radiation efficiency of the three antennas and Fig. 15 compares the total efficiency of the three antennas. The results in these two figures were obtained using the three-antenna approach. The results in Fig. 14 illustrate that the monopole antenna (antenna C) has the least ohmic loss of the three antennas and antenna B has the largest ohmic (and possibly dielectric) loss of the three antennas. The results in Fig. 15 illustrate that the monopole antenna (antenna C) has the lowest total efficiency (dominated by the impedance mismatch, as discussed below). This obviously implies that the monopole is the worst impedance matched antenna of the three. This is further illustrated in Fig. 16, where S_{11} for the three antennas are compared. These S_{11} were measured in both the NIST reverberation chamber and the NIST anechoic chamber. The comparison

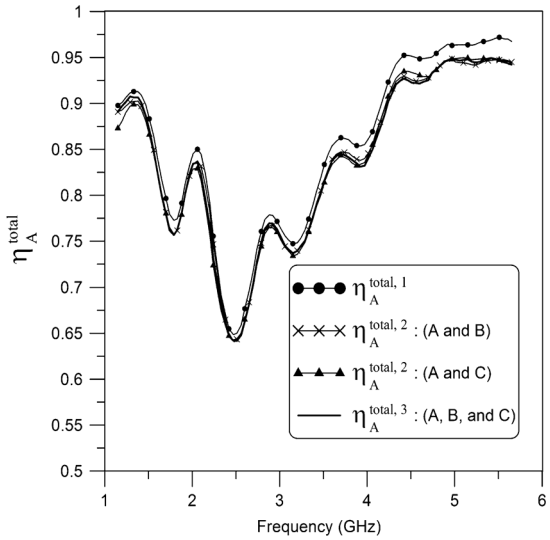

Fig. 11. Total efficiency: a comparison of the three different approaches for antenna A.

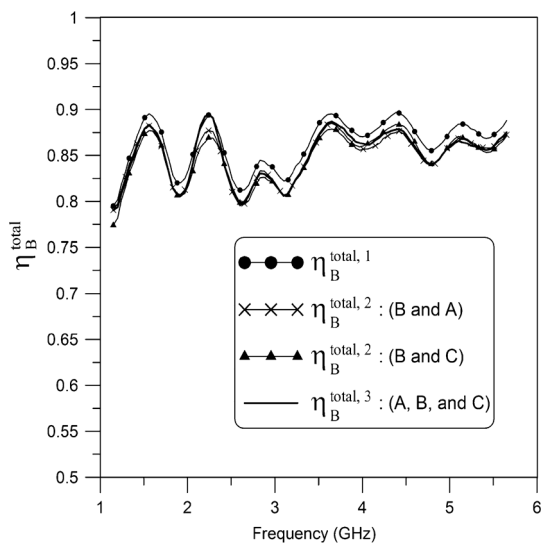

Fig. 12. Total efficiency: a comparison of the three different approaches for antenna B.

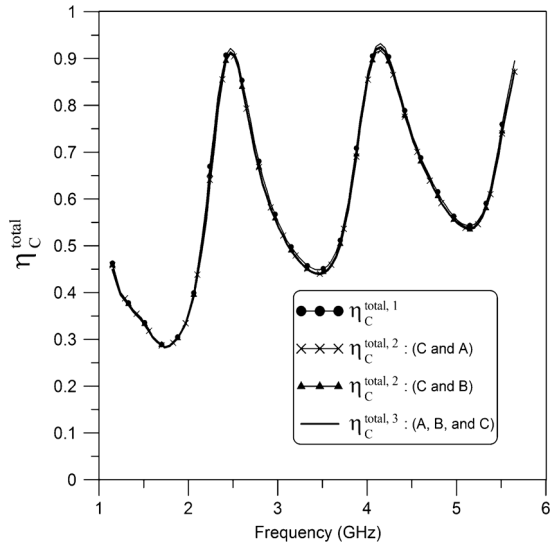

Fig. 13. Total efficiency: a comparison of the three different approaches for antenna C.

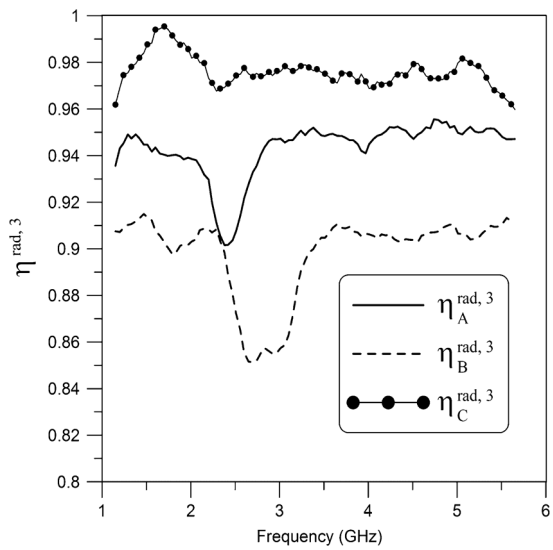

Fig. 14. A comparison of the radiation efficiency for the three antennas measured with the three-antenna approach.

in this figure confirms that the S_{11} measured in a reverberation chamber (averaged over the different independent samples obtained from paddle and frequency averaging, or $|\langle S_{11}\rangle|^2$) is equivalent to an S_{11} measurement performed in an anechoic chamber (i.e., a free-space measurement, or $|S_{11}|^2$). The results in this figure illustrates the poor matching of the monopole antenna (except for the resonances that are inherent in a monopole) when compared to the other two antennas. This figure also illustrates that, on average, antenna B has the best matching behavior.

As stated above, if the chamber is ideal then $e_b = 2$. However, due to imperfections in the chamber performance $e_b \neq 2$. In fact, e_b can be thought of as a quality measure for the chamber performance, the closer that e_b is to 2, the better performing the chamber is (i.e., a well-stirred chamber with a large mode-density). Fig. 17 plots e_b as a function of frequency obtained from the different sets of measurements. We see that e_b is close to 2, but varies as much as 4% from 2. If we look closer at the results in Fig. 8–10, the difference in the one-antenna and two-antenna approach is around 4% as well.

VI. Measurement Uncertainties

In this section, we discuss and estimate the uncertainties associated with these types of antenna efficiency measurements. The Type A and B uncertainties in the measurements are estimated, following the approach described in [20]. For Type A uncertainties related to S-parameter measurements, we use results from earlier work in the same reverberation chamber to obtain an estimate of the uncertainties associated with the calculation of the antenna efficiencies. For an estimate of uncertainties in measuring $\sqrt{\langle |S_{21}|^2\rangle}$, we use the results shown in Fig. 6.1 of [21], which indicates a standard deviation for $\langle |S_{21}|^2\rangle$ of approximately 0.5 dB across the band from 1 GHz to 6 GHz in the unloaded chamber. This standard deviation of $\langle |S_{21}|^2\rangle$ was

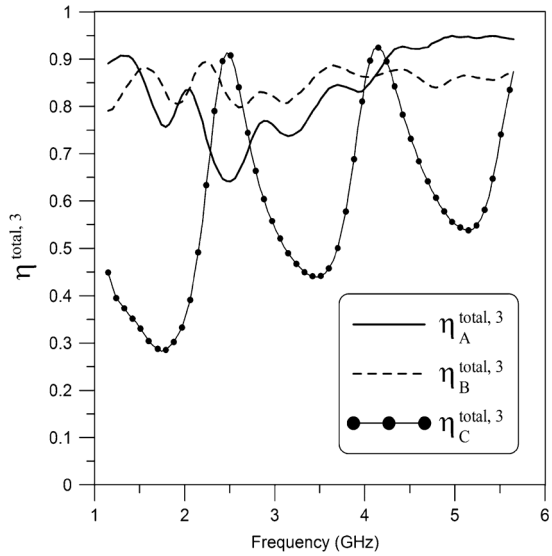

Fig. 15. A comparison of the total efficiency for the three antennas measured with the three-antenna approach.

calculated for 10 different locations in the chamber, where each of the ten $\langle |S_{21}|^2 \rangle$ values was based on 100 different paddle positions. Because we use the same chamber and measurement process, albeit at one location, we anticipate the same uncertainty in our estimate of $\langle |S_{21}|^2 \rangle$. Thus, we use the following for the uncertainty associated with a measurement of $\sqrt{\langle |S_{21}|^2 \rangle}$

$$u_{\sqrt{\langle |S_{21}|^2 \rangle}} = 0.52 \text{ dB}/2 = 0.26 \text{ dB} \tag{42}$$

where the factor of 1/2 is due to the square root. Similar uncertainties are associated with the measurement of $\sqrt{\langle |S_{11}|^2 \rangle}$ and $\sqrt{\langle |S_{22}|^2 \rangle}$.

For Type A uncertainties related to the determination of τ_{RC}, we estimate the uncertainty from the twelve possible combinations, making use of both S_{11} and S_{21} for the different sets of antenna measurements and the two different measurement locations used in the antenna efficiency calculations, see Fig. 7. The relative uncertainty (also referred to as the fractional uncertainty in [23]) with respect to the mean of τ_{RC} for the twelve measurements given in Fig. 7. The relative uncertainty is obtained by summing the mean of τ_{RC} and its standard deviation (from the twelve data sets) normalized by the mean, as defined in [23]. The uncertainties associated with the measurement of the square-root τ_{RC} are

$$u_{\sqrt{\tau_{\mathrm{RC}}}} \leq 0.028 \text{ dB (or} < 0.7\%) \tag{43}$$

across the 1 GHz to 6 GHz band. This is a relative uncertainty. In order to combine or compare uncertainties they must be on the same scale, for which we chose a dB scale. The conversion to a dB scale for τ_{RC} is simply $10\log_{10}$ (relative uncertainty). Since the uncertainty in the square-root τ_{RC} estimation is expected to be much smaller than the uncertainty in $\sqrt{\langle |S_{21}|^2 \rangle}$, $\sqrt{\langle |S_{11}|^2 \rangle}$ and $\sqrt{\langle |S_{22}|^2 \rangle}$ measurements, any significant reduction in Type A uncertainties will need to focus on the S-parameter measurements. In the estimate of the total uncertainty below, we only include the uncertainty in the S-parameter measurements.

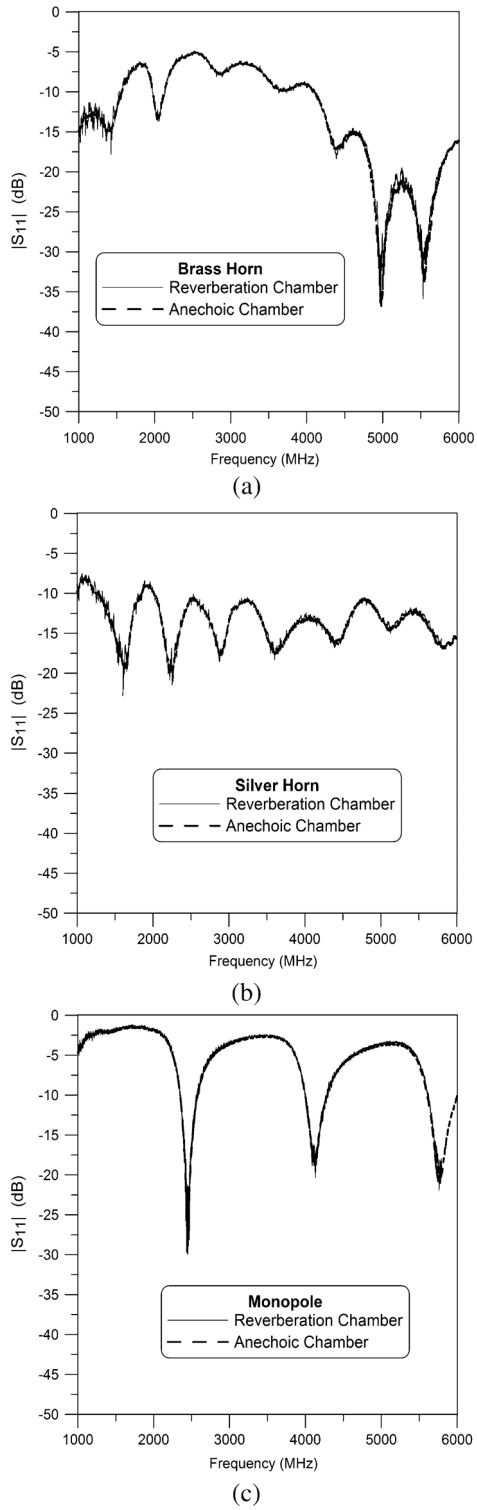

Fig. 16. Reflection or impedance mismatch properties of the three antennas obtained from both reverberation and anechoic chamber measurements: (a) antenna A: brass colored horn, (b) antenna B: silver colored horn, and (c) antenna C: monopole.

The Type A uncertainties stated above are for an unloaded chamber. These Type A uncertainties could possibly be larger if the chamber is loaded with rf absorber (a commonly used practise when testing wireless devices in reverberation chambers [3], [13], and [24]).

TABLE I
SUMMARY FOR THE UNCERTAINTIES FOR THE THREE APPROACHES

uncertainty source		one-antenna	two-antenna	three-antenna
Type A	$u_{\sqrt{\langle \lvert S_{21}\rvert^2\rangle}}$ or $u_{\sqrt{\langle \lvert S_{11}\rvert^2\rangle}}$	0.26 dB	0.26 dB	0.45 dB
	$u_{\sqrt{\tau_{RC}}}$	0.028 dB	0.028 dB	0.048 dB
	Total: Type A	**0.26 dB**	**0.26 dB**	**0.45 dB**
Type B	u_{VNA}	0.2 dB	0.2 dB	0.2 dB
	u_{e_b}	0.09 dB	0.04 dB	—
	Total: Type B	**0.29 dB**	**0.24 dB**	**0.2 dB**
Total	u_C	**0.38 dB**	**0.35 dB**	**0.49 dB**

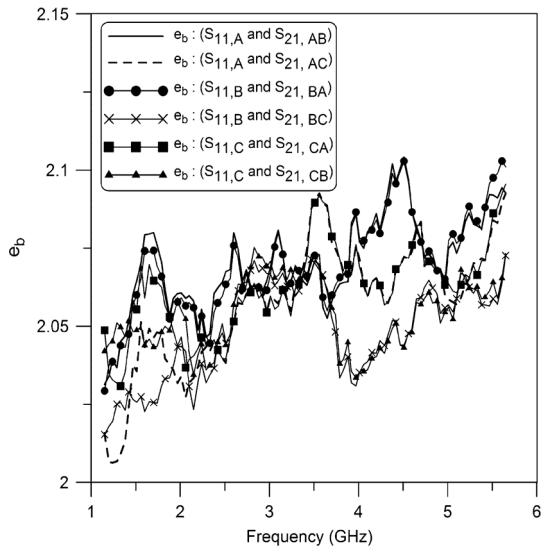

Fig. 17. e_b obtained from different sets of measurements from different two-antenna combinations.

For the Type B uncertainties, we measured the change in the VNA system and cabling setup by measuring $\langle |S_{21}|^2 \rangle$ with a 20 dB attenuator connection between ports 1 and 2 of the VNA four times over an eight-hour time period. This period is larger than the time required to collect all the antenna efficiency data shown in this paper, as well as the time between VNA re-calibrations. The 20 dB attenuator represents an approximation of the loss between antenna pairings in the chamber measurement setup. The difference between the values of $\langle |S_{21}|^2 \rangle$ is less than 0.2 dB for measurements over the eight-hour time period. Thus, we use an uncertainty of the Type B as

$$u_{\mathrm{VNA}} = 0.2\ \mathrm{dB}. \tag{44}$$

This number is consistent with the Type B uncertainties in reverberation chamber measurements reported in [22].

Another source of Type B uncertainty that needs to be included comes from the assumptions inherent in the one-antenna and two-antenna approaches. In these two approaches, it is assumed that the quantity e_b is equal to 2 (the assumption for the one-antenna approach) or it was assumed that e_b is identical for measurements performed in different positions within the chamber (the assumption for the two-antenna approach). This second assumption is a measure of the chamber uniformity. The chamber uniformity and how e_b deviates from 2 are measures of the quality of the RC (where a "good" chamber is well-stirred with a large mode-density), and as such e_b will be different for every chamber (as discussed above, e_b could be used to characterize a chamber). With the limited amount of data presented here, we can only give an estimate of the deviation of e_b from 2. From Fig. 17, the maximum deviation of e_b from 2 is around 4% (or 0.17 dB), and we see the deviation of e_b with position within the chamber is around 2% (or 0.09 dB). Because e_b is under a square-root, we can estimate the Type B uncertainties associated with the $e_b = 2$ assumption for the one-antenna approach is

$$u_{e_b,1} = 0.09\ \mathrm{dB} \tag{45}$$

and we can estimate the Type B uncertainties associated with the uniformity in e_b assumption for the two-antenna approach is

$$u_{e_b,2} = 0.04\ \mathrm{dB} \tag{46}$$

where 1 and 2 correspond in the one-antenna and two-antenna approach. The combined Type B relative uncertainty for the three different techniques is done by the standard manner

$$u_{\mathrm{Type}\ B} = \sqrt{(u_{\mathrm{VNA}})^2 + (u_{e_b})^2}. \tag{47}$$

Note that for the three-antenna approach there is no assumption needed for e_b and hence no uncertainties for this needs to be included.

The standard combined relative uncertainty is then calculated based on the "law of propagation of uncertainty" using the Type A and B uncertainty estimates, as defined in [20]. The combined relative uncertainty for the three approaches can be obtained by

$$u_C = \sqrt{(u_{\mathrm{Type}\ A})^2 + (u_{\mathrm{Type}\ B,1})^2}. \tag{48}$$

The three-antenna approach involve three ratio terms (see (34)), and as such the uncertainties increase by a factor of $\sqrt{3}$. Table I summarizes the uncertainties associated with the three approaches.

Thus, the one-antenna and two-antenna approaches have uncertainties on the order of 9%, and the three-antenna approach has uncertainties on the order of 12%. However, these stated uncertainties are a conservative estimate and the uncertainties are likely less with the use of more averaging (i.e., more independent samples). For example, the type of antenna measurements performed here only require a measurement time of only one to two hours and as such the Type B uncertainties associated with the VNA are closer to 0.1 dB. With this new estimate for $u_{\mathrm{Type}\ B}$, the combined relative uncertainty for the one-antenna approach is $u_C = 0.32$ dB, and the uncertainty for the three-antenna approach is $u_C = 0.46$

dB, or 8% and 11%, respectively. The dominant uncertainty in these measurement methods is associated with the spatial uniformity in the chamber, which shows up in $u_{\sqrt{\langle |S_{21}|^2 \rangle}}$. By increasing the number of independent samples and employing a combination of paddle-averaging, frequency-averaging, and position-averaging (a common practice in RC measurements), the uncertainties can be reduced further to below 10%.

This uncertainty analysis is only for this particular measurement. However, any well-stirred chamber and similar setup should exhibit similar uncertainties. Like our approaches, the uncertainties in the conventional approach discussed in the introduction would be dominated by the uncertainties in the measurement of S_{21}, and as a result we would expect the total uncertainties in the conventional approach would be similar to those discussed above.

VII. Conclusion

In this paper, we presented three new reverberation chamber techniques for determining the efficiency for one, two, and/or three antennas. The commonly used RC techniques for determining the efficiency of an antenna require either the use of a reference antenna (i.e., an antenna with a known efficiency) and/or require one to assume that the two antennas used in the test have identical efficiencies. In this paper we presented techniques that overcome these limitations and assumptions which allow for the determination of both the overall efficiency and radiation efficiency of antennas. We presented a one-antenna approach, a two-antenna approach, and a three-antenna approach. We presented experimental data for three different antennas (one monopole antenna and two different horn antennas). Finally, we discussed the measurement uncertainties associated with the these types of antenna efficiency measurements and conclude that the measurement uncertainties in these RC techniques can be less than 10%.

We are currently investigating the robustness of these three approaches. In particular, we are investigating the ability of these approaches to work when the overall losses in the chamber are dominated by antenna loss and not by chamber losses. We need to emphasize that the techniques presented in this paper assumes that the losses in the chamber are dominated by the chamber wall losses (and possible rf absorber losses if they are used in the chamber, see [13]) when compared to losses in the antennas used in the measurements (i.e., energy pulled out of the chamber by the antennas). When chamber wall losses are not dominant when compare to antenna losses, determining the chamber decay constant (τ_{RC}) can become problematic. When wall losses are not dominant, antenna losses can influence the determination of τ_{RC} (which should only be a parameter of the chamber and not of the antenna). Under these conditions, the techniques presented here need to be modified. Finally, we are also investigating the idea of using e_b as a means to assess the imperfections of a chamber. These topics will be discussed in future publications.

Acknowledgment

The authors thank D. Odum and Dr. V. Rodriguez of ETS-Lindgren for supplying the manufacturer data for antenna B.

References

[1] D. A. Hill, *Electromagnetic Fields in Cavities: Deterministic and Statistical Theories*. New York: IEEE Press, 2009.

[2] P. M. Morse and R. H. Bolt, "Sound waves in rooms," *Rev. Modern Phys.*, vol. 16, no. 2, pp. 69–150, Apr. 1944.

[3] C. L. Holloway, D. A. Hill, J. M. Ladbury, P. Wilson, G. Koepke, and J. Coder, "On the use of reverberation chambers to simulate a controllable Rician radio environment for the testing of wireless devices," *IEEE Trans. Antennas Propag., Special Issue on Wireless Communications*, vol. 54, no. 11, pp. 3167–3177, Nov. 2006.

[4] H. G. Krauthauser and M. Herbrig, "Yet another antenna efficiency measurement method in reverberation chambers," in *Proc. IEEE Int. Symp. on Electromagn. Compat.*, Jul. 25–30, 2010, pp. 536–540.

[5] M. Piette, "Antenna radiation efficiency measurements in a reverberation chamber," in *Proc. Asia-Pacific Radio Science Conf.*, Aug. 24–27, 2004, pp. 19–22.

[6] P.-S. Kildal and K. Rosengren, "Correlation and capacity of MIMO systems and mutual coupling, radiation efficiency and diversity gain of their antennas: Simulations and measurements in reverberation chamber," *IEEE Commun. Mag.*, vol. 42, no. 12, pp. 102–112, Dec. 2004.

[7] A. Khaleghi, "Time-domain measurement of antenna efficiency in reverberation chamber," *IEEE Trans. Antennas Propag.*, vol. 57, no. 3, pp. 817–821, Mar. 2009.

[8] "IEC 61000-4-21: EMC, Part 4: Testing and Measurement Techniques; Section 21: Reverberation Chamber Test Methods," Int. Electrotech. Comm., Geneva, Committee Draft, 2001.

[9] A. A. H. Azremi, H. G. Shiraz, and P. S. Hall, "Reverberation chamber for efficiency measurement of small antennas," in *Proc. Int. Conf. on Computers, Communications, and Signal Processing With Special Track on Biomedical Engineering*, 2005, pp. 25–29.

[10] A. A. H. Azremi, H. G. Shiraz, and P. S. Hall, "Small antenna efficiency by the reverberation chamber and the wheeler cap method," in *Proc. Networks, Jointly Held With the IEEE 7th Malaysia Int. Conf. on Communication*, 2004, pp. 12–16.

[11] P. Hallbjorner, "Reflective antenna efficiency measurements in reverberation chambers," *Microw. Opt. Technol. Lett.*, vol. 30, no. 5, pp. 332–335, 2001.

[12] C. S. Lee, A. Duffy, and C. Lee, "Antenna efficiency measurements in a reverberation chamber without the need for a reference antenna," *IEEE Antennas Wireless Propag. Lett.*, vol. 7, pp. 448–450, 2008.

[13] E. Genender, C. L. Holloway, K. A. Remley, J. M. Ladbury, and G. Koepke, "Simulating the multipath channel with a reverberation chamber: Application to bit error rate measurements," *IEEE Trans. EMC*, vol. 52, no. 4, pp. 766–777, Nov. 2010.

[14] C. L. Holloway, H. Shah, R. J. Pirkl, K. A. Remley, D. A. Hill, and J. Ladbury, "Early-time behavior in reverberation chambers and its effect on the relationships between coherence bandwidth, chamber decay time, rms delay spread, and the chamber build-up time," *IEEE Trans. EMC*, 2012, to be published.

[15] J. M. Ladbury and D. A. Hill, "Enhanced backscatter in a reverberation chamber: Inside every complex problem is a simple solution struggling to get out," in *Proc. IEEE Int. Symp. on Electromagnetic Compatibility*, Jul. 9–13, 2007, pp. 1–5.

[16] J. Ladbury, G. Koepke, and D. Camell, "Evaluation of the NASA Langley Research Center Mode-Stirred Chamber Facility," US Dept. Commerce, Boulder, CO, NIST Tech. Note 1508, Jan. 1999.

[17] J. M. Ladbury and D. A. Hill, "An improved model for antennas in reverberation chambers," in *Proc. IEEE Int. Symp. on Electromagnetic Compatibility*, Jul. 25–30, 2010, pp. 663–667.

[18] C. A. Balanis, *Antenna Theory: Analysis and Design*, 2nd ed. New York: Wiley, 1997, ch. 2.

[19] A. C. Newell, R. C. Baird, and P. F. Wacker, "Accurate measurement of antenna gain and polarization at reduced distances by an extrapolation technique," *IEEE Trans. Antennas Propag.*, vol. 21, no. 4, pp. 418–431, 1973.

[20] B. N. Taylor and C. E. Kuyatt, "Guidelines for Evaluating and Expressing the Uncertainty of NIST Measurement Results," NIST Tech. Note 1297, Sept. 1994.

[21] C. S. Lötbäck Patanè, "Reverberation chamber performance and methods for estimating the Rician K-Factor: Evaluation of Reverberation Chamber Measurements at the National Institute of Standards and Technology in Boulder, Colorado, USA and comparison of methods for estimating the Rician K-Factor in wireless channels," Masters of Science Thesis, Dept. Signals and Systems, Chalmers University of Technology, Gothenburg, Sweden, 2010.

[22] J. B. Coder, J. M. Ladbury, C. L. Holloway, and K. A. Remley, "Examining the true effectiveness of loading a reverberation chamber: How to get your chamber consistently loaded," in *Proc. IEEE Int. Symp. on Electromagnetic Compatibility*, Jul 25–30, 2010, pp. 530–535.
[23] T. R. Taylor, *An Introduction to Error Analysis*, 2nd ed. Sausalito, CA: Univ. Sceince Book, 1997, ch. 2.
[24] C. L. Holloway, D. A. Hill, J. M. Ladbury, and G. Koepke, "Requirements for an effective reverberation chamber: Unloaded or loaded," *IEEE Trans. Electromagn.*, vol. 48, no. 1, pp. 187–194, Feb. 2006.

Christopher L. Holloway (S'86–M'92–SM'04–F'10) received the B.S. degree from the University of Tennessee at Chattanooga, in 1986, and the M.S. and Ph.D. degrees from the University of Colorado at Boulder, in 1988 and 1992, respectively, both in electrical engineering.

During 1992, he was a Research Scientist with Electro Magnetic Applications, Inc., Lakewood, Co. His responsibilities included theoretical analysis and finite-difference time-domain modeling of various electromagnetic problems. From the fall of 1992 to 1994 he was with the National Center for Atmospheric Research (NCAR) in Boulder, Co. While at NCAR his duties included wave propagation modeling, signal processing studies, and radar systems design. From 1994 to 2000, he was with the Institute for Telecommunication Sciences (ITS) at the U.S. Department of Commerce in Boulder, Co., where he was involved in wave propagation studies. Since 2000, he has been with the National Institute of Standards and Technology (NIST), Boulder, CO, where he works on electromagnetic theory. He is also on the Graduate Faculty at the University of Colorado at Boulder. His research interests include electromagnetic field theory, wave propagation, guided wave structures, remote sensing, numerical methods, metamaterials, measurement techniques, and EMC/EMI issues.

Dr. Holloway is a member of URSI Commissions A, B, and E and a Fellow of the IEEE. He is currently serving as Chair for US Commission A of the International Union of Radio Science and is an Associate Editor for the IEEE TRANSACTIONS ON ELECTROMAGNETIC COMPATIBILITY. He was the Chairman for the Technical Committee on Computational Electromagnetics (TC-9) of the IEEE Electromagnetic Compatibility Society from 2000–2005, served as Co-Chair for the Technical Committee on Nano-Technology and Advanced Materials (TC-11) of the IEEE EMC Society from 2006–2011, and served as an IEEE Distinguished lecturer for the EMC Society from 2004–2006.

Haider A. Shah was born in Peshawar, Pakistan, in 1985. He received the B.S. degree in electrical engineering from COMSATS Institute of Information Technology, Islamabad, Pakistan in 2007 and the M.S. degree in electrical engineering (telecommunication) from Chalmers University of Technology, Gothenburg, Sweden, in 2010.

From June 2007 to July 2008, he worked with Nokia Siemens Networks and as a Base Station Sub-System Engineer. He worked as a Guest Researcher at National Institute of Standards and Technology, Boulder, CO. Currently he is working at Ericsson AB, Sweden as a radio performance testing Engineer. His research interest includes wireless communication and signal processing.

Ryan J. Pirkl (S'06–M'10) received the B.S., M.S., and Ph.D. degrees in electrical engineering from the Georgia Institute of Technology, Atlanta, in 2005, 2007, and 2010, respectively.

For his graduate research, he developed hardware, measurement procedures, and processing tools for *in situ* characterization of radio wave propagation mechanisms. In 2010, he began working at the National Institute of Standards and Technology in Boulder, CO under a National Research Council Postdoctoral Research Associateship. He is currently investigating how reverberation chambers may be used as tunable wireless channel emulators for wireless device testing. His research interests include reverberation chambers, radio wave propagation, and analytical electromagnetics.

William F. Young (M'01) received the M.S. degree from Washington State University, Pullman, in 1998 and the Ph.D. degree from the University of Colorado, Boulder, in 2006, both in electrical engineering.

He worked at Sandia National Laboratories from 1998 to 2010, and collaborated with the National Institute of Standards and Technology (NIST) on wireless systems and measurements since 2003. He joined the Electromagnetics Division at NIST in 2010. Hi experience in wireless communication systems includes diversity antenna design, radio frequency propagation measurements, MIMO system applications, electromagnetic interference testing, and wireless network security analysis. He is currently developing radio frequency laboratory measurement techniques that support standards specification efforts by the National Fire Protection Association (NFPA) for Personal Alert Safety Systems (PASS), and by the CTIA-The Wireless Association for Long Term Evolution (LTE) MIMO technology evaluation.

David A. Hill (M'72–SM'76–F'87–LF'08) was born in Cleveland, OH, on April 21, 1942. He received the B.S.E.E. and M.S.E.E. degrees from Ohio University, Athens, in 1964 and 1966, respectively, and the Ph.D. degree in electrical engineering from Ohio State University, Columbus, in 1970.

From 1970 to 1971, he was a Visiting Fellow with the Cooperative Institute for Research in Environmental Sciences, Boulder, CO, where he worked on pulse propagation. From 1971 to 1982 he was with the Institute for Telecommunications Sciences, Boulder, CO, where he worked on antennas and propagation. Since 1982 he has been with the National Institute of Standards and Technology, Boulder, CO, where he works on electromagnetic theory. He is also a Professor Adjoint in the Department of Electrical and Computer Engineering of the University of Colorado, Boulder.

Dr. Hill is a member of URSI Commissions A, B, E, and F and a Life Fellow of the IEEE. He has served as a technical editor for the IEEE TRANSACTIONS ON GEOSCIENCE AND REMOTE SENSING and the IEEE TRANSACTIONS ON ANTENNAS AND PROPAGATION.

John Ladbury (M'09) was born Denver, CO, 1965. He received the B.S.E.E. and M.S.E.E. degrees (specializing in signal processing) from the University of Colorado, Boulder, in 1987 and 1992, respectively.

Since 1987 he has worked on EMC metrology and facilities with the Radio Frequency Technology Division of N.I.S.T. in Boulder, CO. His principal focus has been on reverberation chambers, with some investigations into other EMC-related topics such as time-domain measurements and probe calibrations.

Mr. Ladbury is a member of the International Electrotechnical Commission (IEC) joint task force on reverberation chambers. He has received three "best paper" awards at IEEE International EMC symposia over the last six years.